Radiation Physics and Chemistry 215 (2024) 111376

Contents lists available at ScienceDirect

Radiation Physics and Chemistry

journal homepage: www.elsevier.com/locate/radphyschem

Interactions between X-/gamma rays and alloys used in dental braces: A study on theory and simulations

Ferdi Akman [a,b,*], Hasan Oğul [c], Mehmet Fatih Turhan [d], Cansu Şeyma Ağrılı [e]

[a] Bingöl University, Vocational School of Social Sciences, Department of Property Protection and Security, Program of Occupational Health and Safety, 12000, Bingöl, Turkey
[b] Bingöl University, Central Laboratory Application and Research Center, 12000, Bingöl, Turkey
[c] Sinop University, Faculty of Engineering and Architecture, Department of Nuclear Engineering, Sinop, Turkey
[d] Afyonkarahisar Health Sciences University, Atatürk Vocational School of Health Service, Department of Medical Imaging Techniques, 03200, Afyonkarahisar, Turkey
[e] İstanbul Kent University, Faculty of Dentistry, Department of Orthodontics, 34433, İstanbul, Turkey

ARTICLE INFO

Handling Editor: Piotr Ulanski

Keywords:
Brace
Photon
Radiation shielding
Secondary radiation
Energy deposit

ABSTRACT

In the field of dentistry, the utilization of dental X-rays plays a pivotal role in ensuring accurate diagnoses for various dental conditions. A crucial aspect of this practice involves understanding how these X-ray emissions interact with dental braces. In the presented study, the details of how X-rays and gamma rays interact with different materials used in dental braces, namely stainless steel, nitinol, elgiloy, and beta-titanium alloys, were examined. This investigation was carried out through a combination of advanced simulation codes such as FLUKA and GEANT4, alongside theoretical calculations using the WinXCOM approach. A comprehensive analysis was conducted at fourteen distinct energy levels, ranging from 20 to 150 keV with 10 keV increments. The primary focus of this study revolves around quantifying the shielding characteristics of gamma and X rays as they traverse through these dental brace materials. To achieve this, some gamma/X-ray shielding parameters, buildup-factors, and kerma relative to air were meticulously simulated and calculated. Additionally, the energy deposits within these materials and the subsequent generation of secondary radiations are thoroughly explored. Significantly, these results highlight that elgiloy alloy demonstrates the highest attenuation of X-ray and gamma ray intensities compared to the other considered materials. This comprehensive study thus offers valuable insights into the behavior of dental braces when subjected to ionizing radiation, with potential implications for patient safety and diagnostic accuracy in dental radiology.

1. Introduction

Orthodontic treatment becomes necessary in cases where there is a misalignment of teeth, and a fundamental component of these treatments involves the use of orthodontic arch wires. It is important to note that the selection of orthodontic treatments and the specific types of orthodontic arch wires employed serve a dual purpose. Beyond solely addressing issues related to tooth structure, these treatments also play a crucial role in rectifying disorders within the mandibular structure, in addition to addressing dental misalignments. In essence, orthodontic interventions not only enhance the aesthetics and alignment of teeth but also contribute to the overall improvement of the entire oral and mandibular complex, ensuring both functional and cosmetic benefits for the patient. In this context, there are many common types of wires such as stainless steel, chromium cobalt, nickel titanium and beta-titanium. One of the alloys used in orthodontics for manufacturing brackets, wires, ligatures, bands, and other applications is stainless steel (Arango et al., 2013). Stainless steel alloys have had an important place in orthodontic practice since the 1950s. The most commonly types of stainless steel used in orthodontics are AISI (American Iron and Steel Institute) 302 and 304 (Burstone and Goldberg, 1980; Brantley and Eliades, 2001). These stainless steel alloys contain approximately 70–75% iron, 8% nickel, 18% chromium and 0.20–0.25% carbon. These alloys have good corrosion resistance (Sifakakis and Eliades, 2017). In addition to the formability and flexibility properties of these wires, the low cost made them popular. One of the arch wire materials used in orthodontics during the 1950s is chromium cobalt alloys (elgiloy). This alloy with a nominal composition of 40% cobalt, 20% chromium, 15%

* Corresponding author. Bingöl University, Vocational School of Social Sciences, Department of Property Protection and Security, Program of Occupational Health and Safety, 12000, Bingöl, Turkey.
E-mail address: fakman@bingol.edu.tr (F. Akman).

https://doi.org/10.1016/j.radphyschem.2023.111376
Received 21 July 2023; Received in revised form 6 September 2023; Accepted 27 October 2023
Available online 30 October 2023

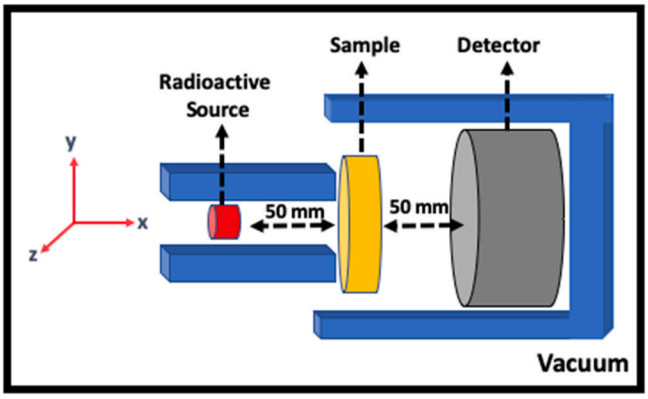

Fig. 1. Typical scheme of geometry where simulations were carried out.

nickel, 7% molybdenum and 16% iron (Burstone and Goldberg, 1980). Chromium cobalt alloys have much lower load-deflection rate (Kuntz et al., 2018). One of the advantages claimed for chromium-cobalt wire over stainless steel is its superior mechanical properties (Philip and Darvell, 2016). These wires are softer than stainless steel wires and also have excellent formability in the soft condition. Chromium cobalt alloys have excellent corrosion resistance. Nickel titanium alloy (nitinol) consists of approximately 52% nickel, 45% titanium and 3% cobalt (Burstone and Goldberg, 1980). Nickel titanium alloy has a become a significant materials because of its advantages such as unique characteristics, including shape memory effect super elasticity and high damping and these alloys are used in many fields such as orthopedics, vascular stents, biomedical field and other medical devices as well as orthodontics (Alipour et al., 2022; Thayer et al., 1995). The application history of beta-titanium wires in orthodontics dates back to the 1980s (Kuntz et al., 2018). Stabilized beta phase titanium alloys contain approximately 80% titanium, 11.5% molybdenum, 6% zirconium and 4.5% tin (Kusy, 1997). Beta-titanium wire has excellent formability and also beta-titanium is the only orthodontic wire alloy possessing true weldability (Brantley and Eliades, 2001).

According to various studies, each choice comes with its unique characteristics, necessitating dentists to make a thoughtful selection. Furthermore, there is a compelling need for further investigation into the interactions of gamma and X-ray radiation. This is imperative to ensure that the right decisions are made, given the potential consequences for both patient safety and the precision of diagnostics in the field of dental radiology. A crucial aspect of this practice involves understanding how these X-ray emissions interact with dental braces. In the presented study, the details of how X-rays and gamma rays interact with different materials used in dental braces were examined. Within this context, a comprehensive assessment of various gamma and X-ray shielding parameters was conducted. Subsequently, an analysis was carried out to identify potential secondary radiations and energy deposits within the selected materials. This is of utmost importance as secondary radiation has the potential to give rise to critical health issues in patients.

Although the gamma/X-rays attenuation parameters are quite limited on the dentistry (Abbasova et al., 2019; Kavaz et al., 2022;

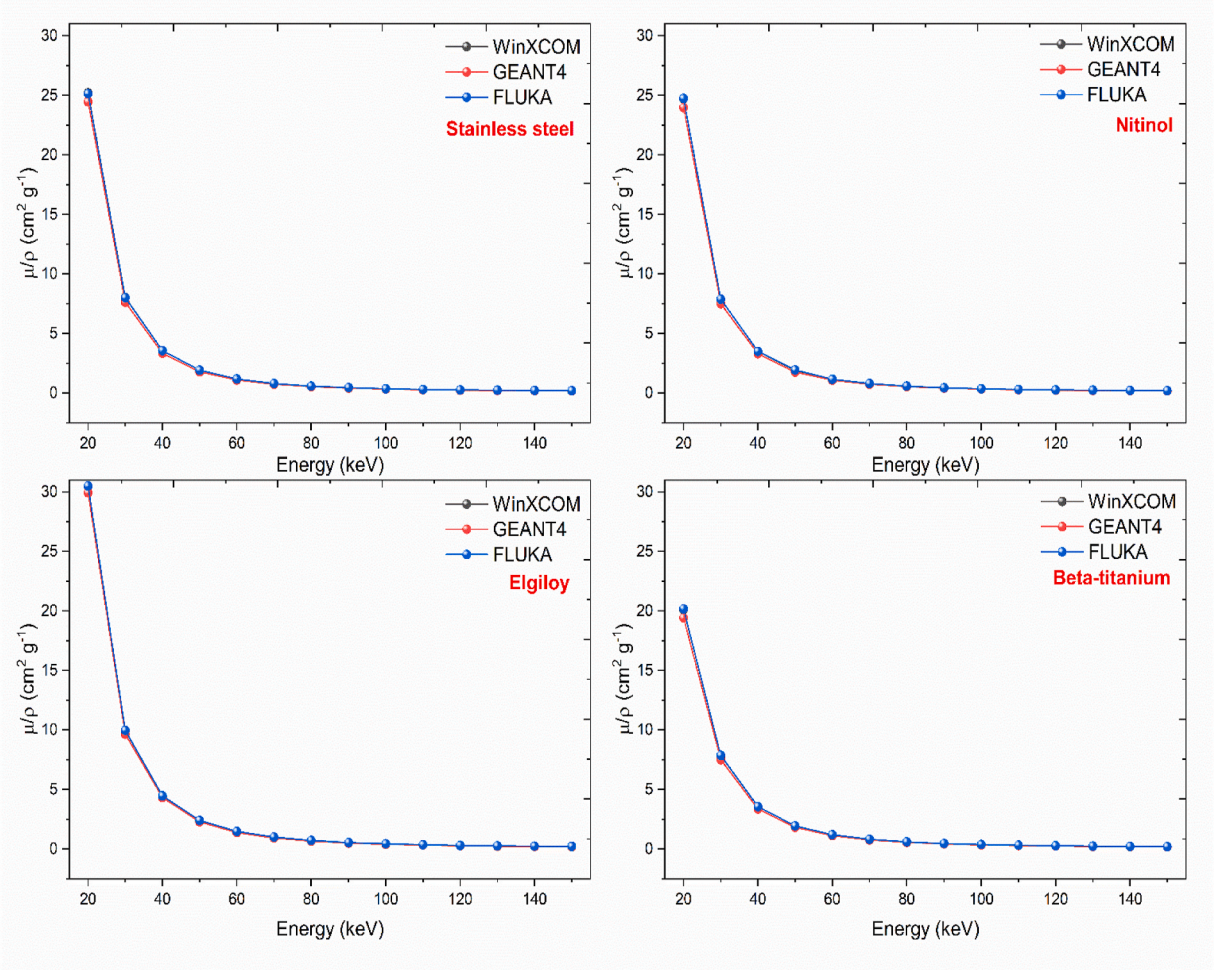

Fig. 2. The graph of μ/ρ-photon energy correlation for the investigated dental braces.

Table 1
The μ/ρ results ($cm^2\ g^{-1}$) calculated with the help of WinXCOM, GEANT4 and FLUKA for the selected dental brace alloys.

Energy (keV)	Stainless Steel			Nitinol			Elgiloy			Beta-Titanium		
	WinX.	GEANT4	FLUKA	WinX.	GEANT4	FLUKA	WinX.	GEANT4	FLUKA	WinX.	GEANT4	FLUKA
20	25.199	24.453	25.137	24.719	23.983	24.732	30.480	29.946	30.490	20.105	19.416	20.180
30	8.020	7.625	8.002	7.885	7.502	7.889	9.944	9.640	9.967	7.845	7.499	7.860
40	3.561	3.343	3.560	3.507	3.294	3.511	4.455	4.321	4.457	3.559	3.361	3.560
50	1.922	1.787	1.924	1.897	1.766	1.939	2.409	2.287	2.411	1.949	1.823	1.952
60	1.184	1.095	1.186	1.170	1.092	1.171	1.476	1.383	1.477	1.212	1.132	1.212
70	0.803	0.740	0.806	0.795	0.733	0.795	0.992	0.920	0.993	0.826	0.769	0.828
80	0.586	0.540	0.588	0.581	0.534	0.582	0.716	0.664	0.716	0.605	0.560	0.610
90	0.453	0.418	0.456	0.450	0.414	0.450	0.546	0.503	0.547	0.468	0.436	0.468
100	0.367	0.339	0.368	0.365	0.336	0.365	0.435	0.402	0.436	0.378	0.352	0.378
110	0.308	0.286	0.310	0.307	0.285	0.307	0.360	0.334	0.360	0.317	0.297	0.317
120	0.267	0.249	0.269	0.266	0.248	0.266	0.307	0.286	0.307	0.273	0.257	0.273
130	0.236	0.222	0.238	0.236	0.222	0.236	0.268	0.251	0.268	0.241	0.228	0.242
140	0.213	0.202	0.214	0.213	0.202	0.213	0.238	0.225	0.239	0.217	0.207	0.217
150	0.195	0.187	0.195	0.195	0.186	0.195	0.216	0.205	0.216	0.198	0.190	0.198

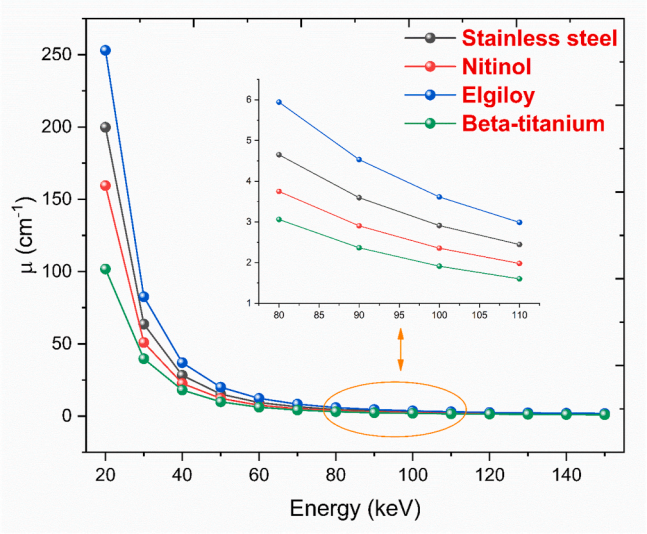

Fig. 3. The graph of μ-photon energy correlation for the investigated dental braces.

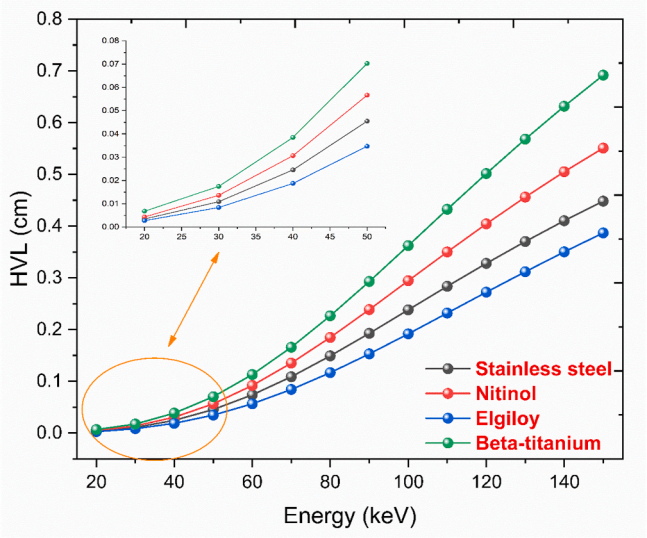

Fig. 4. The graph of HVL-photon energy correlation for the investigated dental braces.

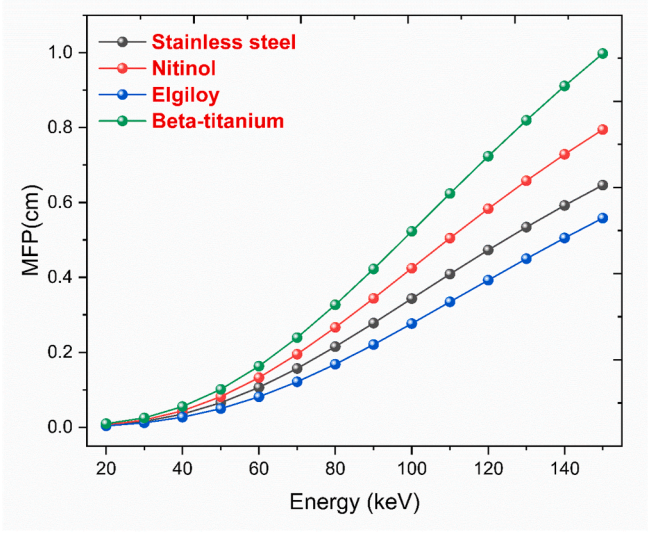

Fig. 5. The graph of MFP-photon energy correlation for the investigated dental braces.

Şengül et al., 2023), studies on the effects of these parameters on various composites (Turhan et al., 2020; Akman et al., 2020; Wu et al., 2022), alloys (Seenappa et al., 2018; Manjunatha et al., 2019; Turhan et al., 2022), ceramics (Akman et al., 2019; Asal et al., 2021; Gharieb et al., 2023), etc. are available in the literature. Abbasova et al. (2019) investigated the gamma ray shielding characteristics of acrylic and zirconium coating materials related to dental applications for nine gamma energies ranging from 122 keV to 1408 keV. Kavaz et al. conducted research to assess the structural and gamma radiation protection characteristics of various dental resin composite materials, including those from 3M, bisco, tokuyama, GC, and kuraray (Kavaz et al., 2022). Besides, Akman et al. reported a study in which they measured various parameters, including the effective atomic number (Z_{eff}), mean free path (MFP), half value layer (HVL), radiation protection efficiency (RPE) and linear attenuation coefficient (μ) for the polyester composition that were filled with varying proportions of CaWO4 and BaTiO3 compounds. These measurements were taken at 22 different energy levels within the range of 0.0595 MeV–1.408 MeV (Akman et al., 2020). Additionally, for Al–Si and Cu–Ag based alloys, Manjunatha et al. (2019) and Turhan et al. (2022) determined the mass attenuation coefficient (μ/ρ), μ, HVL, TVL, MFP, Z_{eff}, effective electron density (N_{eff}), and build-up factors (EABF and EBF). In another study, Asal et al. (2021) reproted the gamma-ray attenuation parameters of the bentonite based ceramic materials.

Table 2
The HVL results (cm) calculated with the help of WinXCOM, GEANT4 and FLUKA for the selected dental brace alloys.

Energy (keV)	Stainless Steel			Nitinol			Elgiloy			Beta-Titanium		
	WinX.	GEANT4	FLUKA	WinX.	GEANT4	FLUKA	WinX.	GEANT4	FLUKA	WinX.	GEANT4	FLUKA
20	0.0035	0.0036	0.0035	0.0043	0.0045	0.0043	0.0027	0.0028	0.0027	0.0068	0.0071	0.0068
30	0.0109	0.0115	0.0109	0.0136	0.0143	0.0136	0.0084	0.0087	0.0084	0.0175	0.0183	0.0174
40	0.0245	0.0261	0.0246	0.0306	0.0326	0.0306	0.0187	0.0193	0.0187	0.0385	0.0408	0.0385
50	0.0455	0.0489	0.0454	0.0566	0.0609	0.0554	0.0347	0.0365	0.0346	0.0703	0.0751	0.0702
60	0.0738	0.0798	0.0737	0.0919	0.0984	0.0918	0.0566	0.0604	0.0565	0.1131	0.1210	0.1130
70	0.1088	0.1182	0.1085	0.1352	0.1467	0.1351	0.0841	0.0908	0.0841	0.1658	0.1782	0.1655
80	0.1491	0.1620	0.1487	0.1848	0.2012	0.1846	0.1167	0.1257	0.1166	0.2265	0.2445	0.2246
90	0.1928	0.2093	0.1917	0.2386	0.2595	0.2386	0.1530	0.1661	0.1528	0.2929	0.3143	0.2928
100	0.2381	0.2579	0.2377	0.2943	0.3196	0.2942	0.1918	0.2076	0.1915	0.3623	0.3896	0.3622
110	0.2835	0.3060	0.2816	0.3500	0.3772	0.3498	0.2319	0.2500	0.2322	0.4324	0.4620	0.4319
120	0.3278	0.3510	0.3249	0.4042	0.4338	0.4038	0.2722	0.2917	0.2720	0.5015	0.5332	0.5012
130	0.3703	0.3937	0.3673	0.4561	0.4841	0.4554	0.3118	0.3327	0.3116	0.5681	0.6006	0.5661
140	0.4104	0.4333	0.4076	0.5051	0.5328	0.5047	0.3502	0.3716	0.3496	0.6317	0.6627	0.6311
150	0.4481	0.4687	0.4478	0.5509	0.5773	0.5511	0.3869	0.4065	0.3867	0.6917	0.7204	0.6908

Table 3
The Z_{eff} results calculated with the help of WinXCOM, GEANT4 and FLUKA for the selected dental brace alloys.

Energy (keV)	Stainless Steel			Nitinol			Elgiloy			Beta-Titanium		
	WinX.	GEANT4	FLUKA	WinX.	GEANT4	FLUKA	WinX.	GEANT4	FLUKA	WinX.	GEANT4	FLUKA
20	25.888	25.121	25.824	25.919	25.147	25.932	28.619	28.118	28.629	25.641	24.762	25.737
30	25.891	24.614	25.832	25.950	24.692	25.966	28.823	27.942	28.888	28.471	27.215	28.526
40	25.886	24.301	25.883	25.949	24.371	25.979	28.887	28.020	28.901	28.695	27.100	28.701
50	25.877	24.060	25.907	25.924	24.132	26.498	28.881	27.417	28.904	28.686	26.834	28.728
60	25.863	23.914	25.910	25.880	24.154	25.908	28.822	26.994	28.834	28.523	26.641	28.532
70	25.845	23.801	25.936	25.824	23.795	25.834	28.722	26.617	28.747	28.234	26.272	28.282
80	25.825	23.769	25.890	25.759	23.659	25.795	28.592	26.538	28.598	27.870	25.823	28.114
90	25.804	23.762	25.948	25.691	23.621	25.689	28.443	26.199	28.476	27.469	25.597	27.481
100	25.783	23.803	25.823	25.622	23.594	25.635	28.286	26.134	28.323	27.058	25.158	27.067
110	25.763	23.868	25.933	25.556	23.716	25.575	28.127	26.088	28.094	26.658	24.952	26.691
120	25.744	24.044	25.974	25.494	23.756	25.524	27.972	26.099	27.990	26.284	24.720	26.296
130	25.726	24.200	25.939	25.438	23.965	25.475	27.825	26.083	27.847	25.941	24.541	26.037
140	25.711	24.354	25.893	25.387	24.064	25.403	27.689	26.094	27.738	25.634	24.436	25.658
150	25.697	24.566	25.711	25.342	24.182	25.331	27.565	26.236	27.576	25.362	24.350	25.395

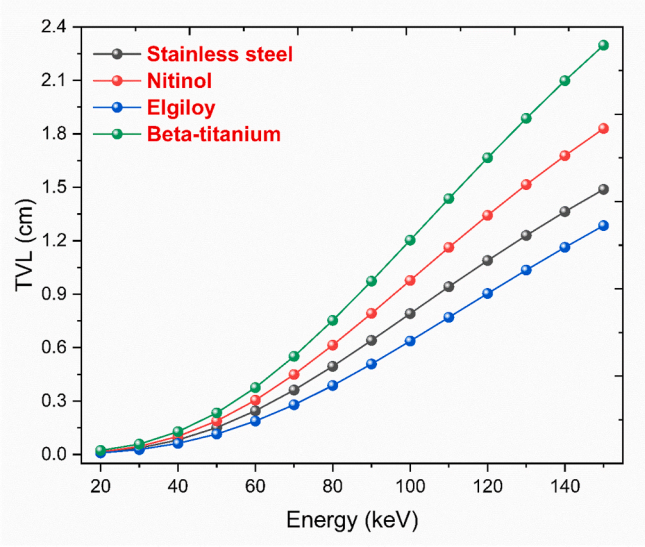

Fig. 6. The graph of TVL-photon energy correlation for the investigated dental braces.

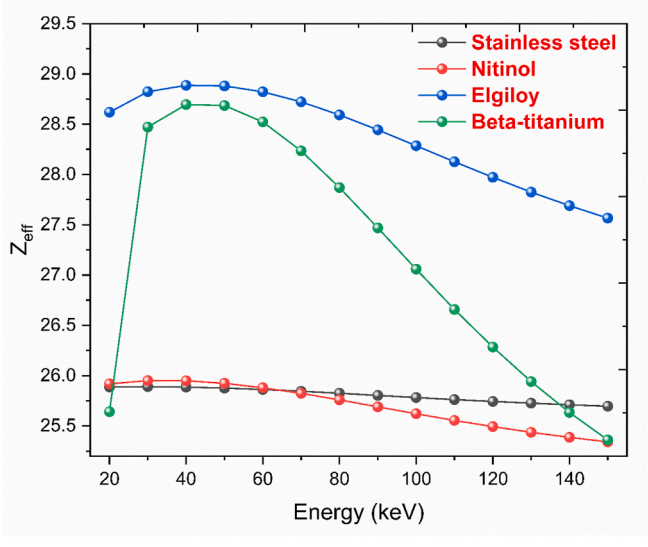

Fig. 7. The graph of Z_{eff}-photon energy correlation for the investigated dental braces.

As could be seen the literature review, there has been a noticeable gap in research concerning the investigation of braced materials in the context of gamma and X-ray interactions. Furthermore, it's noteworthy that many published works have not addressed the occurrence of secondary radiation. Consequently, the study presented here is poised to make a significant contribution to the existing literature by addressing these crucial aspects. This research endeavor is set to play a pivotal role in advancing the evaluation of dental braces. On this purpose, X-/gamma rays attenuation parameters such as μ/ρ, μ, HVL, TVL, MFP and Z_{eff} of orthodontic arch wires (stainless steel, elgiloy, nitinol and beta-

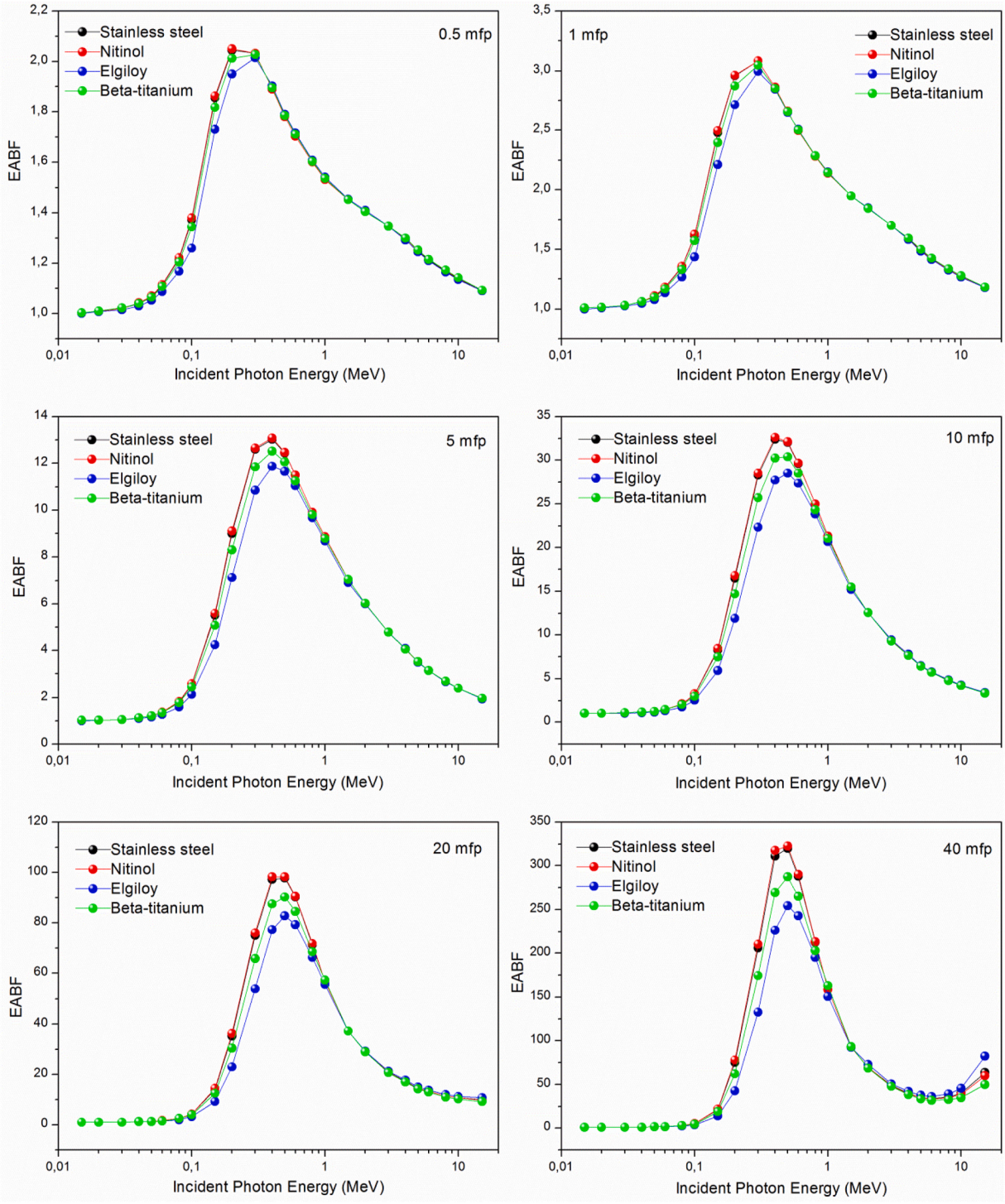

Fig. 8. *EABF* values of the investigated dental braces in the energy region 0.015–15 MeV at 0.5, 1, 5, 10, 20 and 40 *mfp*.

titanium) were firstly determined with WinXCOM, GEANT4 and FLUKA in the range of energy 20 keV $\leq$ E $\leq$ 150 keV. Secondly, exposure buildup factors (EBF) and energy absorption build-up factors (EABF) were evaluated in various energies and for different penetration depths. Secondary radiations and energy deposits results were further examined. Finally, in this particular study, the investigation of kerma relative to air values was carried out across the energy range of 1 keV–20 MeV.

2. Materials and methods

2.1. Processes performed with GEANT4, FLUKA and WinXCOM

This work uses WinXCOM (Gerward et al., 2004) (theoretical method) and GEANT4 (Agostinelli et al., 2003) – FLUKA (Böhlen et al., 2014) packages (Monte Carlo simulations) in order to determine the Gamma/X-rays interactions with alloys used in dental braces, namely stainless steel (density: 7.93 g/cm^3), nitinol (density: 6.45 g/cm^3), elgiloy (density: 8.30 g/cm^3), and beta-titanium (density: 5.06 g/cm^3). WinXCOM code is a useful option to obtain Gamma/X-rays mass

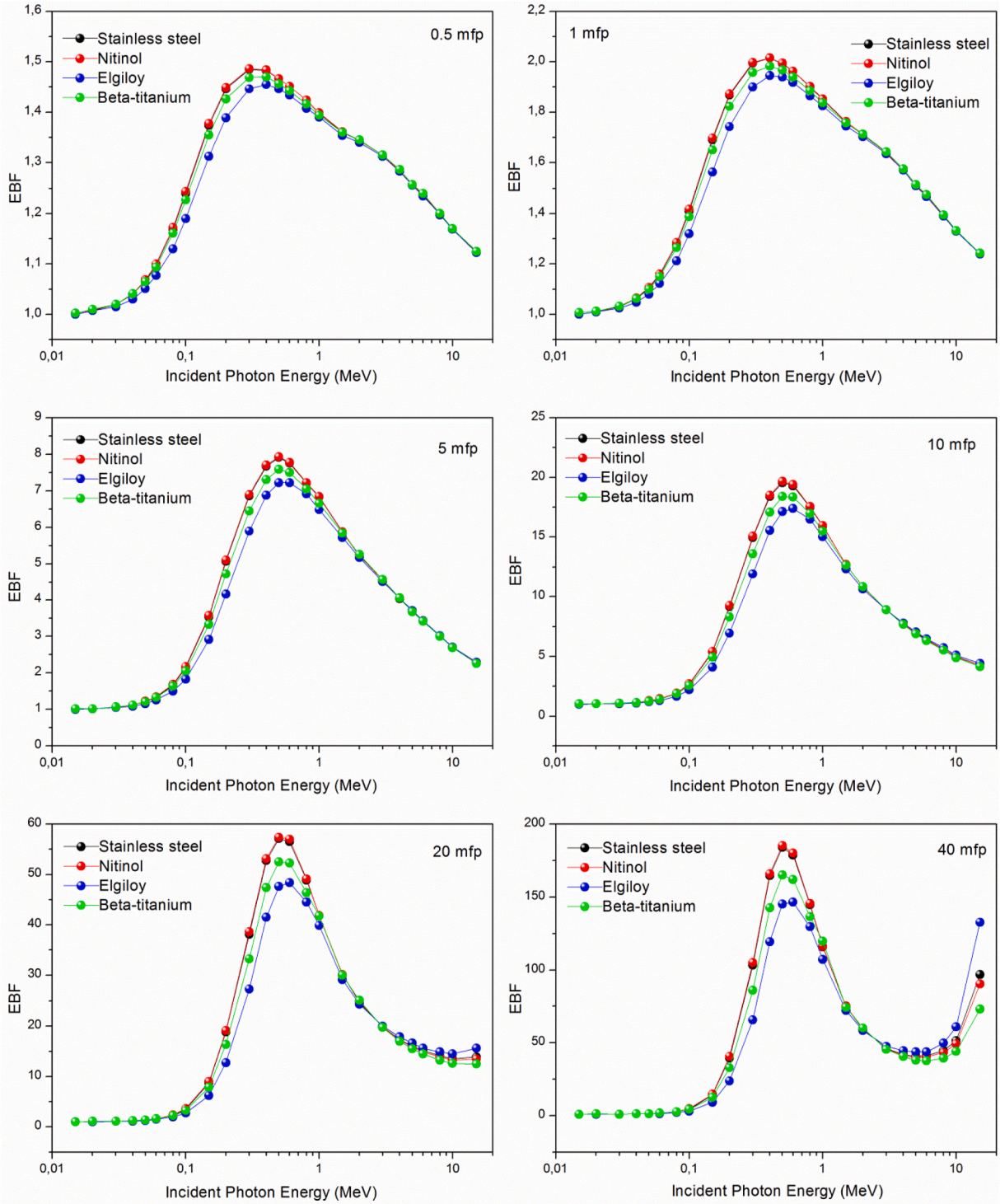

Fig. 9. *EBF* values of the investigated dental braces in the energy region 0.015–15 MeV at 0.5, 1, 5, 10, 20 and 40 *mfp*.

attenuation coefficients of the considered materials at certain energies. In this context, WinXCOM was developed to generate attenuation coefficient or photon interaction cross section of the user defined substance by using predefined μ/ρ values and cross sections for the elements. Its consistency with experimental results and Monte Carlo Simulations (MC) were previously examined, and remarkable agreements were reported (Ozkalaycı et al., 2020; Oğul et al., 2022; Ogul; Gultekin and Ogul, 2023; Aşkin et al., 2020). Therefore, it could be safely considered that WinXCOM provides reliable results.

On the other hand, MC simulations are also useful tools to evaluate the photon interactions with materials in certain circumstances such as lack of experimental apparatus or budget. On this regard, the chosen MC simulations for the presented paper draft are FLUKA and GEANT4 codes. Here, it should be noted that MCNP is a widely used computer program for simulating the behavior of particles in a system. However, it is not freely available to public. Therefore, FLUKA and GEANT4 packages are chosen in the presented study. The accuracy of the software packages was previously verified by comparing the simulated outcomes with both experimental data and the MCNP simulation program (Aşkin et al., 2020; Frosio et al., 2021). FLUKA is a general-purpose simulation

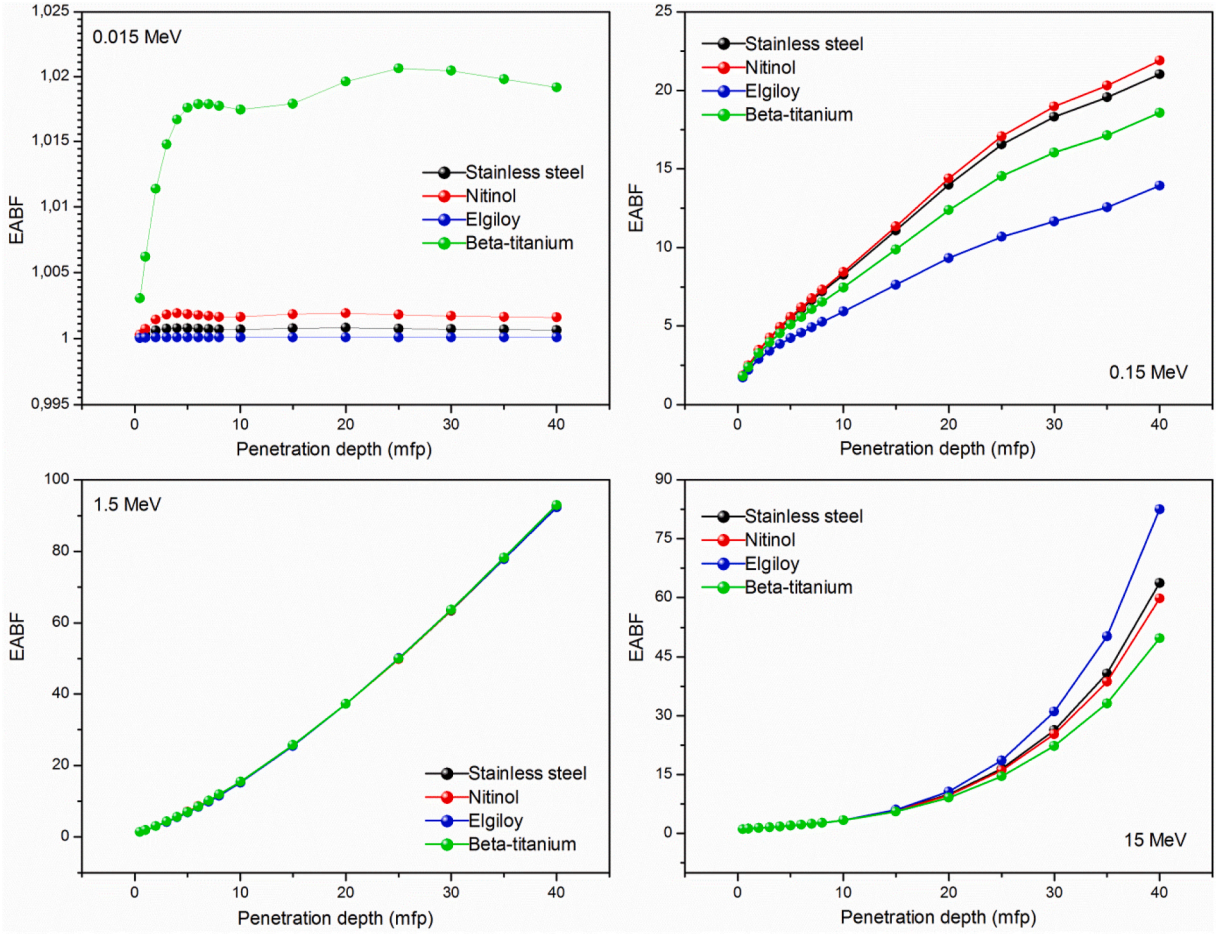

Fig. 10. *EABF* values of the investigated dental braces up to 40 *mfp* at 0.015, 0.15, 1.5, 15 MeV.

package to calculate particle interactions with user defined materials. Here, complex geometries could be even modelled and about 60 different particles might be studied. In our case, the chosen particle interactions, X-/gamma-rays interactions, could be investigated in a wide energy band ranging from 1 keV to thousands of TeV. Similarly, GEANT4 simulation toolkit is also useful choice in order to assess the passage of particles through the user defined materials. As it could be done in FLUKA, the user of GEANT4 can model and create own geometries. Fig. 1 illustrates the schematic view of the simulation geometry studied in this paper. The X-rays interactions are evaluated in vacuum medium in order to avoid external interactions. Mono energetic Gamma/X-rays at the desired energies are sent over the chosen sample only in x-direction. In other words, the chosen material was bombarded with 10,000,000 Gamma/X-rays at desired energy, and then, the transmitted Gamma/X-rays photons through the sample were further determined. With help of simulation of transmitted particles, linear attenuation coefficient (cm^{-1}), mass attenuation coefficient (cm^2/g), half value layer (cm), mean free path (cm), tenth value layer (cm) were calculated.

Additionally, with help of GEANT4 simulation package, the energy deposits in the chosen alloys and the secondary radiation due to the interaction of gamma/X-rays with the materials were investigated. For each gamma/X-rays energy, the average energies of secondary particles were also determined. The material thickness was chosen as 1 cm, and the initial radiation particles were set to 10,000,000.

2.2. The theoretical calculation process

There are many parameters such as mass attenuation coefficient (μ/ρ), mean free path (MFP), energy absorption buildup factor (EABF) to investigate the interaction of Gamma/X-rays with matter and the amount of Gamma/X-rays intensity attenuation of the material. Some of these parameters do not depend on the phase state and density of the matter, while others depend on these two variables. Density-dependent parameters are an important indicator of the material's usability in the field of Gamma/X-rays shielding. The first parameter that is independent of the density and investigates the Gamma/X-rays interaction with material is μ/ρ. This parameter can be calculated theoretically with the mixing rule given in Eq. (1) (Akman et al., 2022a);

$$\left(\mu/\rho\right)_{mater.} = \sum W_i \left(\mu/\rho\right)_i \ \left(cm^2\ g^{-1}\right) \tag{1}$$

In Eq. (1), $(\mu/\rho)_i$ is the mass attenuation coefficient of the i. element in the material interacting with the photon and W_i is the weight fraction for the same element. The sum of the weight fractions of the elements in the material is one, i.e. $\Sigma W_i = 1$. The weighted fraction of any element in the material can be calculated by Eq. (2) (Akman et al., 2015);

$$W_i = \frac{n_i A_i}{\sum_j n_j A_j} \tag{2}$$

where, n_i and A_i are the atom number and atomic weight for the i. element, respectively.

The first parameter that depends on the density, which is important for the usability of the material in the field of radiation shielding, is the linear attenuation coefficient (μ) and is related to the μ/ρ and density (ρ) of the material.

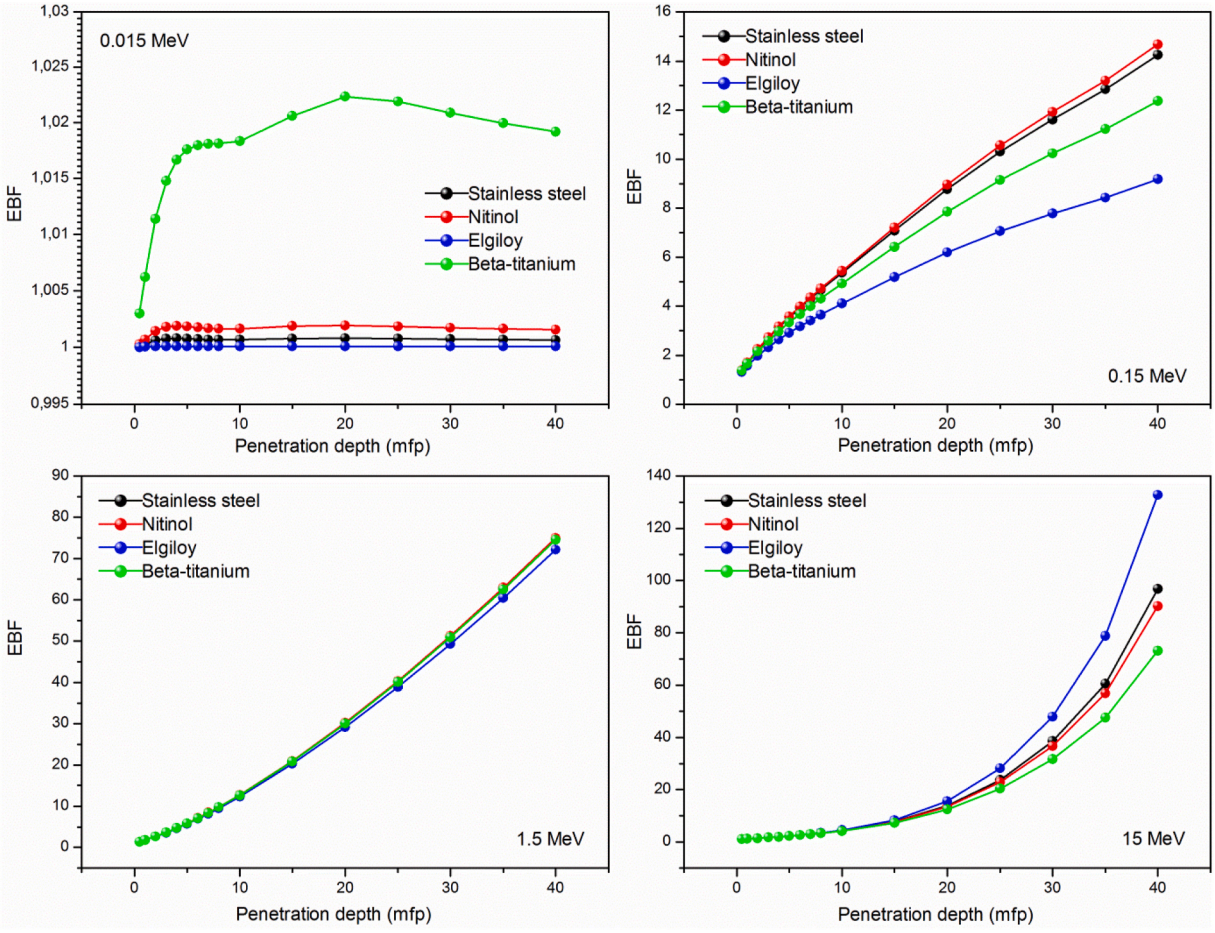

Fig. 11. *EBF* values of the investigated dental braces up to 40 *mfp* at 0.015, 0.15, 1.5, 15 MeV.

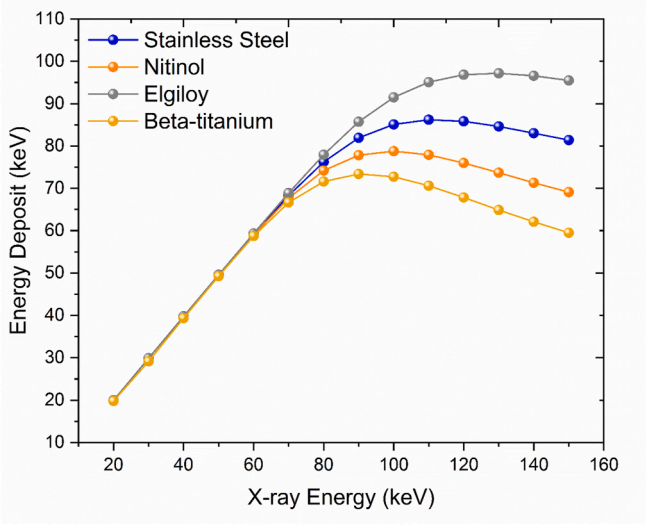

Fig. 12. Energy deposit graphs of the selected alloys at various gamma/X-ray energies.

$$\mu = \frac{\mu}{\rho}\cdot\rho \quad (cm^{-1}) \tag{3}$$

Useful parameters associated with μ are HVL, TVL and MFP. These parameters are the shield thickness needed to attenuate 50%, 90% and 63.2% of the initial radiation intensity value, respectively and can be determined with the help of the following equation (Akman et al., 2022b).

$$HVL = \frac{ln\,2}{\mu} = \frac{0.693}{\mu} \quad (cm) \tag{4}$$

$$TVL = \frac{ln\,10}{\mu} = \frac{2.303}{\mu} \quad (cm) \tag{5}$$

$$MFP = \frac{1}{\mu} \quad (cm) \tag{6}$$

The parameter that is dimensionless and can be calculated using the atomic cross section ($\sigma_{t,a}$, cm/atom) (Akman et al., 2015) and the electronic cross section ($\sigma_{t,e}$, cm/electron) (Akman et al., 2015) of the material is the effective atomic number and can be determined mathematically by the following equation (Akman et al., 2015).

$$Z_{eff} = \sigma_{t,a}/\sigma_{t,e} \tag{7}$$

The buildup-factor is known as the ratio of the total dose that is collided (the photon is scattered once or more in the substance) and non-collided (no interaction) to the non-collided dose. In the present study, EABF and EBF parameters were calculated using the Geometric Progression (G-P) fitting method in the energy range of 0.015–15 MeV and penetration depths of 0.5, 1, 5, 10, 20 and 40 mfp. According to the present study, EABF is a quantity related to the energy accumulated in the braces, while EBF is a quantity related to the amount of radiation exposed as a result of photon ionization of the air. These two buildup factors were calculated by the process described below.

Firstly, the equivalent atomic number parameter (Z_{eq}), which will be

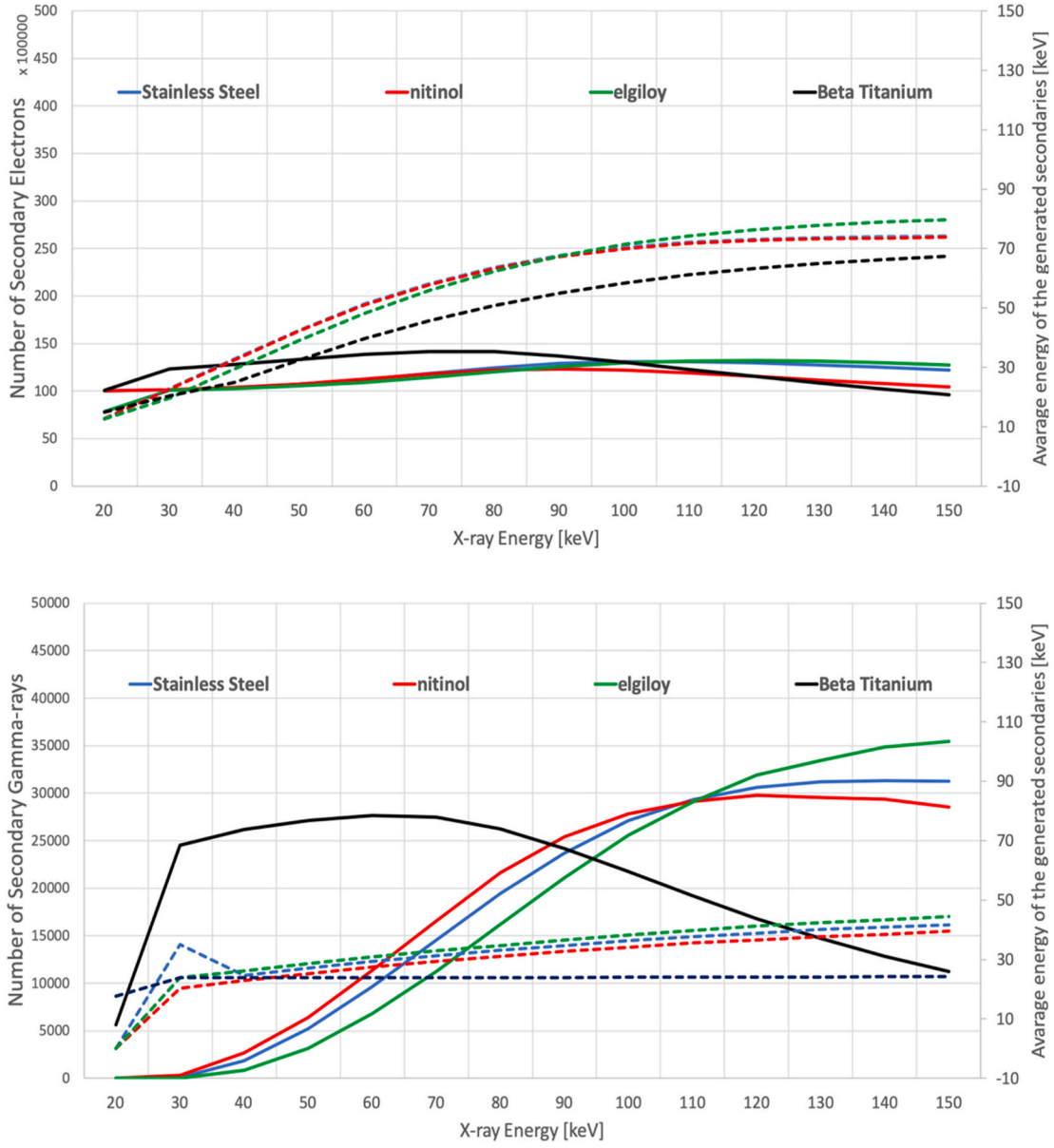

Fig. 13. Generated secondary particles with their average energies.

used in determining the G-P fit parameters, has been calculated. In the determination of this parameter, $(\mu/\rho)_{Compton}$ and $(\mu/\rho)_{Total}$ values obtained from the WinXCOM program were obtained at various energies varying from 15 keV to 15 MeV and for elements between atomic numbers 4 to 40. The corresponding Z_{eq} values of an element with the same energy were calculated from the ratio of these two types of attenuation coefficients. When the R ratio, which is the $(\mu/\rho)_{Compton}/(\mu/\rho)_{Total}$ ratio, is between two consecutive element ratios in the braces, Z_{eq} is calculated using interpolation with the following equation (Turhan et al., 2023);

$$Z_{eq} = \frac{Z_1(log\ R_2 - logR) + Z_2(logR - log\ R_1)}{log\ R_2 - log\ R_1} \tag{8}$$

where, Z_1 and Z_2 are the atomic numbers corresponding to the ratio R_1 and R_2. Using the Z_{eq} values obtained by this process, a, b, c, d and X_K G-P fit parameters were determined with the help of the equation below for the investigated braces (Turhan et al., 2023);

$$P = \frac{P_1(log\ Z_2 - log\ Z_{eq}) + P_2(log\ Z_{eq} - log\ Z_1)}{log\ Z_2 - log\ Z_1} \tag{9}$$

where, P_1 and P_2 are the G-P fit parameters corresponding to atomic numbers Z_1 and Z_2, respectively, and these values for the elements were obtained from the ANSI/ANS-6.4.3 database (ANSI/ANS-6.4.3 and Gamma Ray Attenuation Coefficient, 1991). Using these obtained parameters in the equations below, EABF and EBF parameters were calculated for braces (Turhan et al., 2023).

$$B(E,x) = 1 + \frac{b-1}{K-1}(K^x - 1)\ for\ K \neq 1 \tag{10}$$

$$B(E,x) = 1 + (b-1)x\ for\ K = 1 \tag{11}$$

where, b represents the buildup-factor for 1 mfp penetration depth. The intermediate parameter K specified in Eqs. 10 and 11 is calculated with the following equation (Turhan et al., 2023);

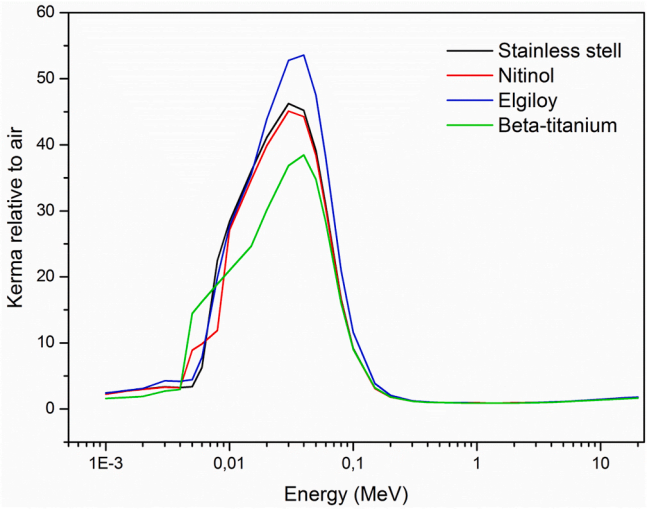

Fig. 14. Kerma relative to air values of the investigated dental braces in the energy region 0.001 MeV–20 MeV.

$$K(E,x) = cx^{a} + d\frac{\tanh\left(\frac{x}{X_K} - 2\right) - \tanh(-2)}{1 - \tanh(-2)} \quad for\ x \leq 40\ mfp \qquad (12)$$

in the equation, x denotes the penetration depth, while E denotes the incident photon energy. The detailed calculation process of kerma relative to air was presented in our previous study (Turhan et al., 2022).

3. Results and discussions

The interactions of the Gamma/X-rays with the considered dental brace alloys were carefully examined using WinXCOM, FLUKA and GEANT4 codes. As motivated earlier, various parameters were considered in these evaluations. The first parameter taken into account is the mass attenuation coefficients. Fig. 2 presents the graph of μ/ρ-photon energy correlation for the investigated dental braces. The graphs show the comparison of WinXCOM, FLUKA and GEANT4 for each chosen material, separately. Also, Table 1 lists the mass attenuation coefficient results of WinXCOM, FLUKA and GEANT4 for the selected dental braces. As could be seen, they agree with each other very well. Here, if the WinXCOM is taken as the reference value, the maximum discrepancy between WinXCOM and GEANT4 is about 7% while the maximum deviation from FLUKA was found to be as about 0.8%. The deviations are negligible but it should be noted here that both software packages employ distinct physics models and databases. Varied nuclear databases and interaction models can lead to different calculations for the interaction of gamma rays with substances. The energy of the X-/gamma-rays is illustrated on x-axes, and it ranges from 20 keV to 150 keV. The obtained values exponentially decrease with increase of the gamma-ray energy. Fig. 3 further provides the graph of μ-photon energy correlation for the investigated dental braces. The dental brace alloys of stainless steel, nitinol, elgiloy and beta-titanium were compared each other. It is clear that better X-/gamma-ray attenuation was obtained with elgiloy material, and stainless steel follow it. Beta-titanium provides worst X-/gamma-ray attenuation characteristics among the chosen materials. The difference between them is clearly greater at lower X-/gamma-ray energies. It should be noted here that the order of materials on μ/ρ values is exactly the same with the order of μ values.

In addition to μ/ρ and μ values, HVL, MFP and TVL quantities are also considered in the presented work. HVL and TVL simply define the required thickness for attenuating half and 9/10 of the incident gamma rays, respectively, while MFP describes the average distance traveled by the radiation without any interaction in the matter. Therefore, consideration of these parameters in the presented work is valuable to conduct a proper and complete conclusion on the considered dental brace alloys. In essence, these parameters are the different form of the μ value and could be easily calculated using obtained linear attenuation coefficients. The graphs of HVL-photon energy correlation, MFP-photon energy correlation and TVL-photon energy correlation for the investigated dental braces are presented in Fig. 4–6, respectively. In addition, the HVL results calculated with the aid of the WinXCOM, FLUKA and GEANT4 methods are presented in Table 2. The lowest HVL value is obtained with elgiloy, which makes it better X-/gamma-rays attenuator among the chosen alloys. MFP and TVL results also confirm that elgiloy dental brace alloy attenuates X-/gamma rays more than others.

The probability of photon interactions with the selected dental brace alloys could be obtained by examining the effective atomic number, Z_{eff}. Table 3 presents the Z_{eff} values calculated with the help of selected methods in the photon energy range of 20–150 keV for the investigated dental brace alloys. Fig. 7 shows the graph of Z_{eff}-photon energy correlation for the investigated dental braces. It is clear that $Z_{eff\ of}$ the beta-titanium alloy is the material mostly affected by the increase of X-/gamma energy. Z_{eff} values of the nitinol and stainless steel show less reaction to increase of X-/gamma-rays energy. The maximum Z_{eff} value was obtained for elgiloy sample. In other words, the X-/gamma-rays interaction possibility with elgiloy is greater than the rest of the selected dental brace alloys.

Fig. 8 shows EABF values of the chosen dental braces in the energy region varying from 0.015 to 15 MeV at 0.5, 1, 5, 10, 20 and 40 mfp while Fig. 9 presents EBF values of the chosen dental braces in the energy region changing from 0.015 to 15 MeV at 0.5, 1, 5, 10, 20 and 40 mfp. We can say from Figs. 8 and 9, Elgiloy exhibits the lowest EABF and EBF values within both the low and intermediate energy ranges. The EABF and EBF values for both the low and intermediate energy regions can be summarized as follows: Nitinol > Stainless Steel > Beta-Titanium > Elgiloy. The range in the high energy region is Elgiloy > Stainless Steel > Nitinol > Beta-Titanium. Also, Figs. 10 and 11 illustrate EABF and EBF values of the investigated dental braces up to 40 mfp at 0.015, 0.15, 1.5, 15 MeV, respectively. As seen from Figs. 10 and **11,** *EABF* and *EBF* values for dental braces were generally increased with increasing penetration depth and energy. While Elgiloy got the lowest *EABF* and *EBF* values at 0.015 MeV, 0.15 MeV and 1.5 MeV, it got the highest *EABF* and *EBF* values in the high energy region at especially penetration depth from 15 *mfp* to 40 *mfp*. This results shows that the photoelectric effect (Z^{4-5}, $E^{-3.5}$), Compton scattering (Z, E^{-1}) and pair production (Z^2, E) are dominant in the low energy region, intermediate energy region and high energy region, respectively.

Charged or neutral particles lose their kinetic energy as they pass through the material due to interactions with the material. This energy loss results in the deposition of energy (dE) within the material. The GEANT4 simulation package is utilized to calculate the energy deposition for each of the materials considered in this study. Fig. 12 illustrates the deposited energy in each material, showing a significant difference between the selected alloys starting at around 80 keV. The elgiloy material exhibits the highest energy deposition, while the beta-titanium alloy shows the lowest energy deposition.

Due to the interaction of gamma-rays with the material, secondary radiations are produced, which could potentially cause damage to living organisms and surrounding materials. GEANT4 MC simulation is used to determine the generated secondary radiations for various X-ray energies, considering electrons and gamma-rays with their average particle energy. Here, the secondary particles are listed as electrons and gamma. The average energy of the secondary electrons ranges from 12 keV to 80 keV, while the energy for gamma-rays varies from 17 keV to 45 keV. It is well-known that gamma-rays, which are ionizing radiation, can be harmful at the mentioned energy levels and should be avoided. Notably, Zheng and Sanche, 2019 [36] reported that electrons with energies ≤30 eV (referred to as low-energy electrons) can damage DNA. The materials considered in this study generate both low-energy

electrons and electrons with energy >30 eV. Therefore, a thorough evaluation of possible secondary particles is crucial. Fig. 13 illustrates the simulated results of the secondary radiations. The solid line represents the number of secondary particles, while the dashed lines indicate their average energies. The top graph of the figure shows the number of secondary electrons with their average energies while the lower panel presents the secondary gamma-rays with their average energies. It should be underlined here that, on the bottom panel of Fig. 13, the results of gamma-ray numbers (shown as a solid black line) for the beta-titanium material are divided by 100 as they exceed the graph's range. In other words, the generated secondary gamma-rays for this material are significantly higher compared to the other three alloys. However, the average energy of the secondary gamma-rays is lower than that of the other three selected samples.

Material selection for gamma-ray shielding depends on a wide variety of factors, and "kerma" value is one of the effects to be considered. Therefore, the last parameter presented in this work is illustrated in Fig. 14, *K* values of the selected dental braces in the energy region changing from 1 keV to 20 MeV. The definition of "kerma" term refers to how much radiation is absorbed or attenuated by a substance. In other words, a high kerma value indicates that gamma radiation is more effectively absorbed or attenuated by the material. This means that the radiation is effectively blocked and the risk of exposure is reduced. If the Kerma value is small, it means that it is less absorbed or attenuated by the material, which can lead to further processing and increased risk of exposure to radiation. In this context, measurement of "kerma" is important for assessing the biological effects of radiation and ensuring the safety of individuals or objects exposed to radiation. While choosing the brace material, the dentist may consider the material with higher kerma value. As seen from Fig. 14, Elgiloy generally took the highest kerma relative to air values. Kerma relative to air values increased with increasing photon energy up to ~400 keV and then tended to decrease with the energy increase. Finally, the values chanced very little in the high energy region. Also, *K* values of the dental braces sharply increase with increasing with photon energy in the low energy region. These sharply increasing occurred about the absorption edge energies of the elements in the Stainless Steel, Nitinol, Elgiloy and Beta-Titanium. Consequently, it could be concluded that *K* values of the Stainless Steel, Nitinol, Elgiloy and Beta-Titanium are depend on the chemical composition of the dental braces.

4. Conclusions

This study presents the results of photon interaction parameters μ/ρ, μ, HVL, MFP, TVL, Z_{eff}, EABF, EBF and kerma relative to air of stainless steel, nitinol, elgiloy and beta-titanium alloys, which are frequently used in dental braces. While some of the parameters were obtained in the gamma/X-ray energy window of 20 keV–150 keV (WinXCOM, FLUKA and GEANT4 methods were used in this energy range), some of them were calculated in a wide energy range to observe the changes in more detail. The X-/gamma rays attenuation characteristics of the selected dental braces were investigated with these calculated parameters. It is observed from the related figures or tables that the variation of μ/ρ results against photon energy decreases exponentially, while HVL, MFP and TVL results increase exponentially against photon energy. Due to the definition of HVL, MFP and TVL, we could accept that a higher mass attenuation coefficient implies a thinner HVL (or TVL) is needed for the same level of radiation attenuation, while a lower mass attenuation coefficient requires a thicker HVL (or TVL) to achieve the same level of attenuation. Here, it is well known fact that the higher the mass attenuation coefficient, the greater the likelihood of gamma radiation interacting with matter. In this context, it is safe to state that elgiloy material is the best gamma-ray shielding material between the considered materials in the presented study. The worst gamma-ray shielding was found for beta-titanium material. It should be underlined that there is a significant difference between the best (elgiloy) and the worst (beta-titanium) gamma-ray attenuator materials. At 20 keV, elgiloy shows 1.5 times better shielding effectiveness than beta-titanium sample while this difference decreases by the energy decrease. For the remaining energies, the elgiloy material shows about 1.2 times bigger μ/ρ values. The μ and Z_{eff} parameters also generally have the same tendency as μ/ρ. The Z_{eff} value is used to estimate the material's ability to interact with gamma rays. These interactions can reduce the energy and intensity of gamma rays, thereby protecting people and equipment from radiation exposure. Therefore, elgiloy, due to its higher Z_{eff} value, could have more gamma-ray interactions compared to other considered materials. Also, it has been reported that there is an almost Gaussian distribution between the EABF, EBF and kerma relative to air parameters and the photon energy. The measurement of "kerma" is important for assessing the biological effects of radiation and ensuring the safety of individuals or objects exposed to radiation. While choosing the brace material, the dentist may consider the material with higher kerma value. In the presented work, elgiloy generally took the highest kerma relative to air values, which is in agreement with previous considered gamma-ray shielding materials. Similarly, according to EABF and EBF, the same dental braces alloy is a better X-/gamma rays attenuator than the others. EEBF takes into account the interactions of gamma rays within the material and the resulting dose rates, whereas EABF is a factor used to measure the absorption of gamma rays within a material. It is desirable for these factors to be large since larger factors means that gamma rays interact more within the material and lose more energy as they are absorbed. Additionally, it should be definitely noted here that the interaction of gamma/X-rays creates hazardous secondary radiations. The possible secondary particles are determined as electrons with average energy of <80 keV and gamma-rays with average energy of <45 keV. It is highlighted that a thorough evaluation of possible secondary particles is crucial. The dentist should interested in dental braces with low secondary radiations. Therefore, the presented data contains important information for dental braces, especially in the X-ray process in dentistry. In addition, this important information can be used in the protection of living things and/or electronic equipment in nuclear power generation plants, space studies and all work areas where these rays are used, which are important for shielding X- or gamma rays.

Author statement

Ferdi Akman: Conceptualization, Formal analysis, Writing-Review&Editing, Supervision, Project administration.

Hasan Oğul: Methodology, Validation, Investigation, Resources, Data Curation, Writing-Original Draft.

Mehmet Fatih Turhan: Methodology, Investigation, Resources, Writing-Review&Editing, Data Curation.

Cansu Şeyma Ağrılı;: Writing-Original Draft, Writing-Review&Editing, Methodology.

Declaration of competing interest

The authors declare that they have no known competing financial interests or personal relationships that could have appeared to influence the work reported in this paper.

Data availability

Data will be made available on request.

References

Abbasova, N., Yüksel, Z., Abbasov, E., Gülbiçim, H., Tufan, M.Ç., 2019. Investigation of gamma-ray attenuation parameters of some materials used in dental applications. Results Phys. 12, 2202–2205.

Agostinelli, S., Allison, J., Amako, K., Apostolakis, J., Araujo, H., Arce, P., Asai, M., Axen, D., Banerjee, S., Barrand, G., Behner, F., Bellagamba, L., Boudreau, J., Broglia, L., Brunengo, A., Burkhardt, H., Chauvie, S., Chuma, J., Chytracek, R.,

Cooperman, G., 2003. Geant4-a simulation toolkit. Nucl. Instrum. Methods Phys. Res. 506, 250–303. https://doi.org/10.1016/S0168-9002(03)01368-8.
Akman, F., Durak, R., Turhan, M.F., Kaçal, M.R., 2015. Studies on effective atomic numbers, electron densities from mass attenuation coefficients near the K edge in some samarium compounds. Appl. Radiat. Isot. 101, 107–113.
Akman, F., Khattari, Z.Y., Kaçal, M.R., Sayyed, M.I., Afaneh, F., 2019. The radiation shielding features for some silicide, boride and oxide types ceramics. Radiat. Phys. Chem. 160, 9–14.
Akman, F., Kaçal, M.R., Almousa, N., Sayyed, M.I., Polat, H., 2020. Gamma-ray attenuation parameters for polymer composites reinforced with $BaTiO_3$ and $CaWO_4$ compounds. Prog. Nucl. Energy 121, 103257.
Akman, F., Ogul, H., Ozkan, I., Kaçal, M.R., Agar, O., Polat, H., Dilsiz, K., 2022a. Study on gamma radiation attenuation and non-ionizing shielding effectiveness of niobium-reinforced novel polymer composite. Nucl. Eng. Technol. 54 (1), 283–292.
Akman, F., Ozkan, I., Ozel, F., Aydemir, H., Kaçal, M.R., Agar, O., 2022b. Production of barite-doped yarns and testing their usability for ionizing and electromagnetic radiation shielding. Radiat. Phys. Chem., 110464
Alipour, S., Taromian, F., Ghomi, E.R., Zare, M., Singh, S., Ramakrishna, S., 2022. Nitinol: from historical milestones to functional properties and biomedical applications. Proc. Inst. Mech. Eng. H 236 (11), 1595–1612.
ANSI/ANS-6.4.3, Gamma Ray Attenuation Coefficient and Buildup Factors for Engineering Materials, 1991. American Nuclear Society, La Grange Park, IL.
Arango, S., Peláez-Vargas, A., García, C., 2013. Coating and surface treatments on orthodontic metallic materials. Coatings (3), 1–15.
Asal, S., Erenturk, S.A., Haciyakupoglu, S., 2021. Bentonite based ceramic materials from a perspective of gamma-ray shielding: preparation, characterization and performance evaluation. Nucl. Eng. Technol. 53, 1634–1641.
Aşkin, A., Mutuwong, C., Nutaro, T., Dal, M., 2020. Investigation of the radiation shielding capability of xPbO–(50−x)BaO–50B2O3 glass system using Geant4, fluka, WinXCOM and comparison of data with the experimental data. Pramana - J. Phys. 94, 11. https://doi.org/10.1007/s12043-019-1890-4.
Böhlen, T.T., Cerutti, F., Chin, M.P.W., Fassò, A., Ferrari, A., Ortega, P.G., Mairani, A., Sala, P.R., Smirnov, G., Vlachoudis, V., 2014. The FLUKA code: developments and challenges for high energy and medical applications. Nucl. Data Sheets 120, 211–214. https://doi.org/10.1016/j.nds.2014.07.049.
Brantley, W.A., Eliades, T., 2001. Orthodontic materials scientific and clinical aspects. Thieme 77–100.
Burstone, C.J., Goldberg, A.J., 1980. Beta titanium: a new orthodontic alloy. Am. J. Orthod. 77 (2), 121–132.
Frosio, T., Bertreix, P., Menaa, N., Thomas, S., 2021. Calculation and benchmark of fluence-to-local skin equivalent dose coefficients for neutrons with FLUKA, MCNP, and GEANT4 Monte-Carlo codes. J. Radiol. Prot. 41 (3), 564.
Gerward, L., Guilbert, N., Jensen, K., Levring, H., 2004. WinXCom - a program for calculating X-ray attenuation coefficients. Radiat. Phys. Chem. 71, 653–654. https://doi.org/10.1016/j.radphyschem.2004.04.040.
Gharieb, M., Kenawy, S.H., El-Bassyouni, G.T., Hamzawy, E.M.A., 2023. Gamma ray and fast neutron shielding of $ZrSiO_4$-Al_2O_3 ceramic refractor. Part. Sci. Technol. 41 (2), 250–260.
Gultekin, B., Ogul, H., 2023. Evaluation of Acrylonitrile Butadiene Styrene (ABS) polymer reinforced with Bi and TiO_2 nanopowders for gamma and neutron shielding. Radiochim. Acta 111 (2), 137–145. https://doi.org/10.1515/ract-2022-0081.
Kavaz, E., Tekin, H.O., Zakaly, H.M.H., Issa, S.A.M., Kara, U., Al-Buriahi, M.S., Salah, S., Matori, K.A., Zaid, M.H.M., 2022. Structural and gamma-ray attenuation properties of different resin composites for radiation shielding applications. Braz. J. Phys. 52 (157), 1–9.
Kuntz, M.L., Vadori, R., Khan, M.I., 2018. Review of superelastic differential force archwires for producing ideal orthodontic forces: an advanced technology potentially applicable to orthognathic surgery and orthopedics. Curr. Osteoporos. Rep. 16, 380–386.
Kusy, R.P., 1997. A review of contemporary archwires: their properties and characteristics. Angle Orthod. 67 (3), 197–207.
Manjunatha, H.C., Sathish, K.V., Seenappa, L., Gupta, D., Alfred Cecil Raj, S., 2019. A study of X-ray, gamma and neutron shielding parameters in Si- alloys. Radiat. Phys. Chem. 165, 108414.
H. Ogul. Radiation attenuation properties of polymer composites mixed with tantalum carbide, Radiat. Eff. Defect Solid, 177:5–6, 531-544, DOI: 10.1080/10420150.2022.2063124..
Oğul, H., Polat, H., Akman, F., Kaçal, M.R., Dilsiz, K., Bulut, F., Agar, O., 2022. Gamma and Neutron Shielding Parameters of Polyester-based composites reinforced with boron and tin nanopowders. Radiat. Phys. Chem. 201, 110474 https://doi.org/10.1016/j.radphyschem.2022.110474.
Ozkalaycı, F., Kaçal, M.R., Agar, O., Polat, H., Sharma, A., Akman, F., 2020. Lead (II) chloride effects on nuclear shielding capabilities of polymer composites. Phys. Chem. Solids 145, 109543. https://doi.org/10.1016/j.jpcs.2020.109543.
Philip, S.M., Darvell, B.W., 2016. Effect of heat treatment on the tensile strength of 'Elgiloy' orthodontic wire. Dent. Mater. 32, 1036–1041.
Seenappa, L., Manjunatha, H.C., Sridhar, K.N., Hanumantharayappa, C., 2018. Gamma and X-ray radiation compatibility of Ti–Ta–Hf–Zr alloys used for coronary stent applications. Nucl. Sci. Tech. 29 (3), 1–7.
Şengül, A., Akkurt, İ., Gunoglu, K., Akgüngor, K., Ermis, R.B., 2023. Experimental evaluation of gamma-rays shielding properties of ceramic materials used in dentistry. Radiat. Phys. Chem. 204, 110701.
Sifakakis, I., Eliades, T., 2017. Adverse reactions to orthodontic materials. Aust. Dent. J. 62, 20–28.
Thayer, T.A., Bagby, M.D., Moore, R.N., DeAngelis, R.J., 1995. X-ray diffraction of nitinol orthodontic arch wires. Am. J. Orthod. Dentofacial Orthop. 107 (6), 604–612.
Turhan, M.F., Akman, F., Polat, H., Kaçal, M.R., Demirkol, İ., 2020. Gamma-ray attenuation behaviors of hematite doped polymer composites. Prog. Nucl. Energy 129, 103504.
Turhan, M.F., Akman, F., Taşer, A., Dilsiz, K., Oğul, H., Kaçal, M.R., Ağar, O., 2022. Gamma radiation shielding performance of $Cu_xAg_{(1-x)}$-alloys: experimental, theoretical and simulation results. Prog. Nucl. Energy 143, 104036.
Turhan, M.F., Akman, F., Kaçal, M.R., Polat, H., Demirkol, İ., 2023. A study for gamma-ray attenuation performances of barite filled polymer composites. Appl. Radiat. Isot. 191, 110568.
Wu, Z., Li, Y., Yan, Q., Liu, G., Liu, Y., Wang, G., He, L., 2022. Gamma radiation shielding properties of WO_3/Bi_2O_3/waterborne polyurethane composites. J. Kor. Phys. Soc. 81, 199–205.
Zheng, Y., Sanche, L., 2019. Clustered DNA damages induced by 0.5 to 30 eV electrons. Int. J. Mol. Sci. 20 (15), 3749.